2734–2747 Nucleic Acids Research, 2007, Vol. 35, No. 8 Published online 10 April 2007
doi:10.1093/nar/gkm179

Selective use of multiple vitamin D response elements underlies the 1α,25-dihydroxyvitamin D_3-mediated negative regulation of the human *CYP27B1* gene

Mikko M. Turunen, Thomas W. Dunlop, Carsten Carlberg and Sami Väisänen*

Department of Biochemistry, University of Kuopio, FIN-70211 Kuopio, Finland

Received December 15, 2006; Revised and Accepted March 12, 2007

ABSTRACT

The human 25-hydroxyvitamin D_3 ($25(OH)D_3$) 1α-hydroxylase, which is encoded by the *CYP27B1* gene, catalyzes the metabolic activation of the $25(OH)D_3$ into 1α,25-dihydroxyvitamin D_3 ($1\alpha,25(OH)_2D_3$), the most biologically potent vitamin D_3 metabolite. The most important regulator of *CYP27B1* gene activity is $1\alpha,25(OH)_2D_3$ itself, which down-regulates the gene. The down-regulation of the *CYP27B1* gene has been proposed to involve a negative vitamin D response element (nVDRE) that is located ~500 bp upstream from transcription start site (TSS). In this study, we reveal the existence of two new VDR-binding regions in the distal promoter, 2.6 and 3.2 kb upstream from the TSS, that bind vitamin D receptor–retinoid X receptor complexes. Since the down regulation of the *CYP27B1* gene is tissue- and cell-type selective, a comparative study was done for the new $1\alpha,25(OH)_2D_3$-responsive regions in HEK-293 human embryonic kidney and MCF-7 human breast cancer cells that reflect tissues that, respectively, are permissive and non-permissive to the phenomenon of $1\alpha,25(OH)_2D_3$-mediated down-regulation of this gene. We found significant differences in the composition of protein complexes associated with these *CYP27B1* promoter regions in the different cell lines, some of which reflect the capability of transcriptional repression of the *CYP27B1* gene in these different cells. In addition, chromatin architecture differed with respect to chromatin looping in the two cell lines, as the new distal regions were differentially connected with the proximal promoter. This data explains, in part, why the human *CYP27B1* gene is repressed in HEK-293 but not in MCF-7 cells.

INTRODUCTION

The biologically active form of vitamin D, 1α, 25-dihydroxyvitamin D_3 ($1\alpha,25(OH)_2D_3$)), is required for mineral homeostasis and skeletal integrity, as well as controlling cell growth and differentiation in several tissues (1). In the body, the amount of $1\alpha,25(OH)_2D_3$ is tightly controlled by several enzymes that are transcribed from genes belonging to the cytochrome P450 (CYP) family. This gene family encodes a wide variety of enzymes that are needed in the oxidative metabolism of a number of endogenous and exogenous compounds (2). One of the enzymes needed in the metabolism of $1\alpha,25(OH)_2D_3$ is the protein product of the *CYP27B1* gene, 25-hydroxyvitamin D_3 ($25(OH)D_3$) 1α -hydroxylase. It has an important role in the synthesis of $1\alpha,25(OH)_2D_3$ because it catalyzes the metabolic activation of the main circulating form of vitamin D, $25(OH)D_3$, into $1\alpha,25(OH)_2D_3$ (3). *CYP27B1* gene expression is negatively regulated by $1\alpha,25(OH)_2D_3$, and this has been proposed to occur via a negative vitamin D response element (nVDRE), located ~500 bp upstream from transcription start site (TSS) (4). The down-regulation of this gene by $1\alpha,25(OH)_2D_3$ is a cell-type and tissue-restricted phenomenon. In the body, the major expression site of the *CYP27B1* gene and its protein product, $25(OH)D_3$ 1α-hydroxylase (CYP27B1), is the kidney. Within this organ, both the mRNA and the protein product have been observed to be repressed in the presence of $1\alpha,25(OH)_2D_3$ in the proximal tubules only (5). The *CYP27B1* gene is also expressed in extra renal sites (6), however the suppression of the gene by $1\alpha,25(OH)_2D_3$ has been described only in a few other cell lines derived from other tissues, such as colon-derived cells (7).

The effects of $1\alpha,25(OH)_2D_3$ are mediated via the vitamin D receptor (VDR), a member of the nuclear receptor superfamily, to which $1\alpha,25(OH)_2D_3$ binds with high affinity. Responsiveness of a given gene to $1\alpha,25(OH)_2D_3$ requires that its regulatory regions contain

*To whom correspondence should be addressed. Tel:+358-17-163064; Fax: +358-17-2811510; Email: vaisanen@messi.uku.fi

a VDRE. The VDREs of positively regulated genes are direct repeats of two hexameric-core-binding motifs spaced by 3 or 4 nt (DR3 or DR4, respectively) or everted repeats spaced by 6–9 nt (ER6 and ER9, respectively) (8,9). The hexameric sequences of the response elements of the primary $1\alpha,25(OH)_2D_3$ target genes usually have the consensus sequence RGKTSA (R = A or G, K = G or T, S = C or G). The VDREs of most previously studied negatively regulated genes resemble those of positively regulated genes, although negative regulation may not necessarily require both VDRE half sites (10–12). The reported negative VDRE of the *CYP27B1* is an exception, because it does not contain a consensus sequence (4). In addition, the authors proposed that the regulation of the *CYP27B1* gene involves an indirect binding of VDR to DNA, where VDR associates with the nVDRE ligand-dependently via another transcription factor, the VDR interacting repressor (VDIR).

Binding of $1\alpha,25(OH)_2D_3$ causes a conformational change within the ligand-binding domain of the VDR, which modulates its interactions with nuclear proteins, such as coactivator (CoA) and corepressor (CoR) proteins (13). CoR proteins, such as NCoR1 (14) and SMRT/NCoR2 (15), link non-liganded, DNA-bound VDR to enzymes with histone deacetylase activity that cause chromatin condensation (16). The conformational change within VDR's ligand-binding domain results in the replacement of a CoR by a CoA protein of the p160 family, such as SRC-1, SRC-2 or SRC-3 (17). These CoAs link the ligand-activated VDR to enzymes displaying histone acetyltransferase (HAT) activity, such as CBP, that cause chromatin relaxation by their action on histone tails and thereby reversing the action of unliganded VDR (18).

Traditionally, VDREs are thought to locate relatively close to the TSS of $1\alpha,25(OH)_2D_3$ target genes. For example, both human and rat vitamin D 24-hydroxylase (*CYP24*) genes have a cluster of VDREs in their proximal promoters (approximate position −140 to −300) (19–22). However, recently several promoter studies have revealed that the gene promoters may contain multiple response elements that locate not only within proximal promoters but also in more distal regions (23,24) and even within coding regions (25,26). These studies have so far concerned with only positively regulated genes. This raises a question, whether negatively regulated genes also have multiple response elements. Since the promoter studies of the human *CYP27B1* gene have so far been limited to the first 1.7 kb upstream of the TSS (4,27–29), in this study, we have extended the promoter analysis further upstream and examined the role of distal promoter regions to the regulation of the human *CYP27B1* gene by $1\alpha,25(OH)_2D_3$. We analyzed 13 contiguous genomic regions spanning 5.4 kb of the *CYP27B1* promoter by chromatin immunoprecipitation (ChIP) scanning. Our studies revealed two new $1\alpha,25(OH)_2D_3$-responsive regions in the distal promoter 2.6 and 3.2 kb upstream from the TSS. Interestingly, in contrast to the nVDRE-containing region, *in silico* screening revealed that both of the new $1\alpha,25(OH)_2D_3$-responsive regions contained classical VDRE sequences that were shown to directly bind VDR–retinoid X receptor (RXR) heterodimers in a ligand-dependent manner, when studied by gel shift assays. Extensive ChIP analysis suggested that the new regions have a number of similarities with the established nVDRE in the recruitment of different cofactors, as well as recruiting both VDR and RXR, supporting the idea that the putative VDREs are functional. In addition, chromatin conformation capture (3C) analysis suggested that the new regions are directly connected with the TSS via chromatin looping in a ligand-dependent and cell-specific manner.

MATERIALS AND METHODS

Cell culture

HEK-293 human embryonic kidney cells and MCF-7 human breast cancer cells were maintained in Dulbecco's modified Eagle medium (DMEM) containing 5% fetal bovine serum (FBS), 2 mM L-glutamine, 0.1 mg/ml streptomycin and 100 U/ml penicillin in a humidified 95% air–5% CO_2 incubator. Before use in experimental procedures, FBS was stripped of lipophilic compounds, such as endogenous nuclear receptor ligands, by stirring it with 5% activated charcoal (Sigma-Aldrich, St. Louis, MO, USA) for 3 h at room temperature. Charcoal was then removed by centrifugation and the media was sterilized by filtration (0.2 μM pore size). Prior to mRNA or chromatin extraction, the cells were grown overnight in phenol red-free DMEM, supplemented with 5% charcoal-stripped FBS, to reach 50–60% confluency. For ChIP assays, the cells were first treated with 2.5 μM α-amanitin (Sigma-Aldrich) for 2 h, followed by exposure to the ligand, after the removal of the α-amanitin. The cells were then treated with either solvent (ethanol, 0.1% final concentration) or with the 10 nM $1\alpha,25(OH)_2D_3$ (kindly provided by Dr Lise Binderup, LEO Pharma, Ballerup, Denmark, diluted in ethanol). For the RNAi analysis, the cells were grown in phenol red-free DMEM supplemented with 5% charcoal-stripped FBS until they reached a confluency of 40–50%.

Total RNA extraction, cDNA synthesis and real-time PCR

Total RNA was extracted using the Mini RNA Isolation II kit (Zymo Research, HiSS Diagnostics, Freiburg, Germany) and cDNA synthesis was performed for 1 h at 37°C using 1 μg of total RNA as a template, in the presence of 100 pmol oligodT_{18} primer and 40 U reverse transcriptase (Fermentas, Vilnius, Lithuania). Real-time quantitative PCR was performed in an IQ-cycler (BioRad, Hercules, CA, USA) using the dye SybrGreen I (Molecular Probes, Leiden, The Netherlands). Per reaction, 0.3 U Hot Start Taq polymerase (Fermentas) and 3 mM $MgCl_2$ were used and the PCR cycling conditions were: 40 cycles of 30 s at 95°C, 30 s at 62°C and 40 s at 72°C. The sequences of the gene-specific primer pairs for the human *CYP24*, *CYP27B1*, *METTL1*, *VDIR* and the reference gene *RPLP0* are listed in Table 1. PCR product quality was monitored using post-PCR melt curve analysis.

Table 1. Primer sequences used in real-time PCR

Gene	Primer sequences
CYP27B1	5′-CAGACAAAGACATTCATGTGGG-3′
	5′-GTTGATGCTCCTTTCAGGTAC-3′
CYP24	5′-CAAACCGTGGAAGGCCTATC-3′
	5′-AGTCTTCCCCTTCCAGGATCA-3′
VDIR	5′-GTGCCAACTGCACCTCAACAG-3′
	5′-AGGTTCCGCTCTCGCACTTG-3′
METTL1	5′-TGCCTACGTGCTAAGAGTTGG-3′
	5′-CTTCACTCAGGTCCTCCAGAG-3′
RPLP0	5′-AGATGCAGCAGATCCGCAT-3′
	5′-GTGGTGATACCTAAAGCCTG-3′

RNAi and immunoblotting

HEK-293 and MCF-7 cells were transfected with either non-specific siRNA oligomers or Stealth™ siRNAs targeting the VDR mRNA (Invitrogen, Carlsbad, CA, USA) by using Lipofectamine 2000 reagent (Invitrogen, Carlsbad, CA, USA) according to the instructions of the manufacturer. The cells were seeded into 6-well plates and grown in phenol red-free DMEM supplemented with 5% charcoal-stripped FBS. Liposomes containing control or VDR siRNA were formed by incubating 100 pmol of each siRNA duplex with 5 µl of Lipofectamine 2000 for 20 min at room temperature in a total volume of 500 µl of phenol red-free DMEM without antibiotics. The liposomes were added to the cells and siRNA treatment was continued for 72 h after which the cells were treated with ethanol or 10 nM $1\alpha,25(OH)_2D_3$ for 3 h. Total RNA extraction, cDNA synthesis and the real time quantitative PCR analysis were done as mentioned above. Silencing of VDR at the protein level was verified by immunoblotting using 25 µg of whole cell extract from HEK-293 or MCF-7 cells and anti-VDR antibody (sc-1008, Santa Cruz Biotechnologies, Heidelberg, Germany). Cellular proteins were separated using 12% SDS polyacrylamide gel electrophoresis. The blotted proteins were detected by using ECF Western Blotting kit according to the manufacturer's guidelines (GE Healthcare Europe, Helsinki, Finland).

DNA constructs

Full-length cDNAs for human VDR (30) and human RXRα (31) were subcloned into the T_7/SV40 promoter-driven pSG5 expression vector (Stratagene, LaJolla, CA, USA). The same constructs were used for both T_7 RNA polymerase-driven *in vitro* transcription/translation of the respective cDNAs and for viral promoter-driven over-expression in mammalian cells. Promoter regions of the *CYP27B1* gene (see Figure 4) were cloned by PCR from human genomic DNA using Pfu DNA polymerase (Fermentas, Vilnius, Lithuania) and were fused with the thymidine kinase (*tk*) promoter driving the firefly luciferase (*Luc*) reporter gene. All constructs were verified by sequencing.

Gel shift analysis

VDR, RXR and VDIR proteins were generated by coupled *in vitro* transcription/translation using their respective pSG5-based cDNA expression constructs and TNT Quick Coupled Transcription/Translation Systems as recommended by the supplier (Promega, Madison, WI, USA). Protein batches were quantified by test translation in the presence of ^{35}S-methionine (see Figure 3B). The specific concentration of the receptor proteins was adjusted to ~4 ng/µl (10 ng corresponds to ~0.2 pmol) after taking the individual number of methionine residues per protein into account. Gel shift assays were performed with 10 ng of the appropriate *in vitro*-translated proteins. The proteins were incubated for 15 min in a total volume of 20 µl of binding buffer (10 mM Hepes (pH 7.9), 150 mM KCl, 1 mM dithiothreitol, 0.2 µg/µl of poly(dI-C), 5% glycerol). Constant amounts (1 ng) of ^{32}P-labeled double-stranded oligonucleotides (50 000 c.p.m.) corresponding to one copy of dimeric response element were then added and incubation was continued at room temperature for 20 min. Protein–DNA complexes were resolved by electrophoresis through non-denaturing 8% (w/v) polyacrylamide gels in 0.5× TBE (45 mM Tris, 45 mM boric acid, 1 mM EDTA, pH 8.3) and quantified on an FLA-3000 reader (Fuji, Tokyo, Japan) using Image Gauge software (Fuji, Tokyo, Japan). Oligonucleotides were labeled by a Klenow fragment DNA polymerase (Fermentas, Vilnius, Lithuania)-mediated filling in reaction in the presence of a nucleotide mixture containing radiolabeled ^{32}P α-dCTP.

ChIP assays

ChIP assays were performed as previously described (24). The antibodies against acetylated histone H3 (AcH3, 06-599) and H4 (AcH4, 06-866) were from Upstate Biotechnology (Lake Placid, NY, USA). IgG (sc-2027) and the antibodies against VDR (sc-1008), RXR (sc-553), CBP (sc-369), phosphorylated RNA polymerase II (pPol II, sc-13583), SRC-1 (sc-7216), SRC-2 (sc-8996), SRC-3 (sc-7216), Sin3A (sc-5378), SMRT/NCoR2 (sc-1610) and NCoR1 (sc-8994) were obtained from Santa Cruz Biotechnologies. The ChIP templates were analyzed by semi-quantitative real-time PCR. For each of the 13 regions of the human *CYP27B1* promoter, primer pairs were designed (Table 2), optimized and controlled by running PCR with 25 ng genomic DNA (input) as a template. When running immunoprecipitated DNA (output) as a template, the following PCR profile was used: pre-incubation for 5 min at 95°C, 38 cycles of 30 s at 95°C, 30 s at a primer-specific annealing temperature and 30 s at 72°C and one final incubation for 10 min at 72°C. The PCR products were separated by electrophoresis through 2% agarose gels. Gel images were scanned on an FLA-3000 reader (Fuji, Tokyo, Japan) and analyzed using Image Gauge software (Fuji, Tokyo, Japan).

3C analysis

Prior to 3C analysis, the ligand treatment, formaldehyde crosslinking and collection of the HEK-293 and MCF-7

Table 2. PCR primers used in ChIP analysis

Region No.	Location	Primer sequences
1	+20 to −370	5′-CGCGAAAGAAAGCGCTTCTC-3′ 5′-GGGGAATTCCTGAGGATGGG-3′
2	−350 to −776	5′-CCCATCCTCAGGAATTCCCC-3′ 5′-GCTGCTAACCAGAAAGCCCC-3′
3	−756 to −1278	5′-GGGGCTTTCTGGTTAGCAGC-3′ 5′-GAGTTGCAGTGGGGAATGAG-3′
4	−1258 to −1681	5′-CTCATTCCCCACTGCAACTC-3′ 5′-GGACCATAGGGGATCTTTGG-3′
5	−1661 to −1961	5′-CCAAAGATCCCCTATGGTCC-3′ 5′-GTCCTCCAGGCAGTGACCTC-3′
6	−1941 to −2506	5′-GAGGTCACTGCCTGGAGGAC-3′ 5′-GCCTACGTGCTAAGAGTTGG-3′
7	−2486 to −2885	5′-CCAACTCTTAGCACGTAGGC-3′ 5′-GTGTGCAGTGGAACTGTCAC-3′
8	−2865 to −3090	5′-GTGACAGTTCCACTGCACAC-3′ 5′-CATGTATCCTCAGCCCTCCC-3′
9	−3070 to −3462	5′-GGGAGGGCTGAGGATACATG-3′ 5′-GTCCAGTTCTGCCTGGGCAC-3′
10	−3442 to −3907	5′-GTGCCCAGGCAGAACTGGAC-3′ 5′-CTGGTGACATCAGCATGGAG-3′
11	−3928 to −4444	5′-CCATGCTGATGTCACCAG-3′ 5′-CAGGTCAGCGTTTATGGG-3′
12	−4426 to −5049	5′-CCCATAAACGCTGACCTG-3′ 5′-CAGAGGGAGAGAGAGGAG-3′
13	−5031 to −5433	5′-GTCTCGGCTGCCATGATC-3′ 5′-CGAGACCAGGAGTAAGGG-3′

Sequences and location relative to the TSS (+1) are shown.

Table 3. PCR primer sequences used in 3C analysis

Region	Location	Primer sequences
A	−8 to −29	5′-CATATCTCAACCCCTATTTAAC -3′
B	−1652 to −1671	5′-GGATCTTTGGAAGGCTGTG-3′
C	−2661 to −2679	5′-CTGGTGGGTTAGGCTGGT-3′
D	−3222 to −3241	5′-GTTCCAGTTCTGCCCCTTC-3′

Sequences and location relative to the *CYP27B1* gene TSS are shown.

cells were done as described for the ChIP analysis. After harvesting of the cells by centrifugation, the cell pellets were resuspended in 3C lysis buffer 1 (5 mM PIPES, pH 8.0, 85 mM KCl, 0.5% NP-40, protease inhibitors) and the nuclei were collected by centrifugation and washed once with ice-cold PBS. The pellets were resuspended in 3C lysis buffer 2 (1× PBS, 1% NP-40, 0.5% sodium deoxycholate, 0.1% SDS, protease inhibitors). Cellular debris was removed by centrifugation and the lysates were divided into 200 µl aliquots. The aliquots were diluted by adding 150 µl of sterile water and 40 µl of 10× digestion buffer (50 mM Tris-HCl (pH 7.5), 10 mM $MgCl_2$, 100 mM NaCl, 0.1 mg/ml BSA) and 100 U of HinfI restriction enzyme (Fermentas). The samples were incubated overnight at 37°C after which 50 U of T4 DNA ligase (Fermentas) and rATP (final concentration of 0.5 mM, Fermentas) were added. The samples were incubated for 1 h at room temperature and then 2 µl of proteinase K (10 mg/ml, Fermentas) was added and the samples were further incubated overnight at 64°C. Finally, the DNA was recovered by phenol–chloroform extraction followed by ethanol precipitation and analyzed by PCR using primers which are listed in Table 3.

Cell transfections and luciferase reporter gene assays

HEK-293 and MCF-7 cells were seeded into 6-well plates (10^5 cells/ml) and grown overnight in phenol red-free DMEM supplemented with 5% charcoal-stripped FBS. Plasmid DNA containing liposomes were formed by incubating a reporter plasmid and the expression vector for human VDR (each 1 µg) with 10 µg *N*-[1-(2,3-dioleoyloxy)propyl]-*N*,*N*,*N*-trimethylammonium methylsulfate (DOTAP, Roth, Karlsruhe, Germany) for 15 min at room temperature in a total volume of 100 µl. After dilution with 900 µl phenol red-free DMEM, the liposomes were added to the cells. Here, 500 µl of phenol red-free DMEM supplemented with 15% charcoal-stripped FBS was added 4 h after transfection. At this time, either 100 nM $1\alpha,25(OH)_2D_3$ or solvent was also added. The cells were lysed, 16 h after onset of stimulation, using reporter gene lysis buffer (Roche Diagnostics, Mannheim, Germany). The constant light signal luciferase reporter gene assay was performed as recommended by the supplier (Canberra-Packard, Groningen, The Netherlands). Luciferase activities were normalized with respect to protein concentration and induction factors were calculated as the ratio of luciferase activity of ligand-stimulated cells to that of solvent controls.

RESULTS

Expression profiling of CYP27B1 gene expression in response to $1\alpha,25(OH)_2D_3$

To establish model systems, in which to study the expression level and the transcriptional responsiveness of the *CYP27B1* gene, we have chosen the cell line HEK-293, which was derived from a tissue (kidney) where this gene is known to be regulated by $1\alpha,25(OH)_2D_3$. As a reference, we took the cell line MCF-7, which is often used to study $1\alpha,25(OH)_2D_3$ signaling, but in which the *CYP27B1* gene is not regulated by $1\alpha,25(OH)_2D_3$. The expression of the *CYP27B1* gene and its response to $1\alpha,25(OH)_2D_3$ was studied by real-time quantitative PCR (Figure 1A). As a control, the methyltransferase-like-1 (*METTL1*) gene, a direct genomic neighbor of the *CYP27B1* gene, was studied in case the hormone also regulated its transcription. Moreover, the levels of the *VDIR* gene were examined, because of its key role in the regulation of *CYP27B1* gene (4). Finally, the *CYP24* gene, which is known to be strongly up-regulated in the presence of $1\alpha,25(OH)_2D_3$, was used as a positive control for the presence of the hormone. In HEK-293 cells, the *CYP27B1* mRNA expression was significantly down-regulated after 6 and 24 h treatment with $1\alpha,25(OH)_2D_3$. In contrast, in MCF-7 cells, *CYP27B1* mRNA expression was not affected by $1\alpha,25(OH)_2D_3$ treatment. This non-responsive effect of MCF-7 cells has already been observed before (32). The expression of *METTL1* mRNA did not change in MCF-7 cells but in HEK-293 cells a transient down

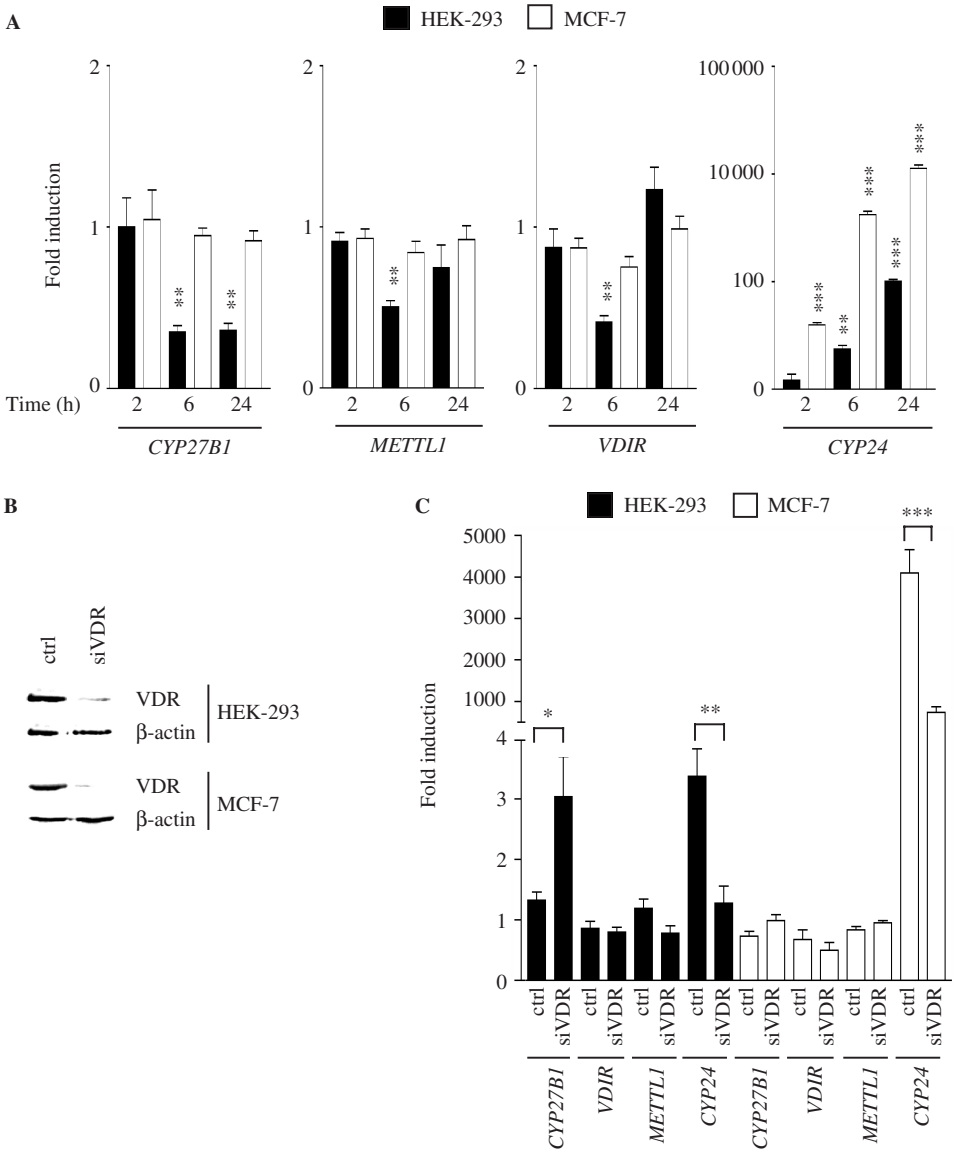

Figure 1. Expression profiling of the human genes *CYP27B1*, *METTL1*, *VDIR*, and *CYP24*. Quantitative real-time PCR was performed in order to study the relative mRNA expression levels of the genes *CYP27B1*, *METTL1*, *VDIR* and *CYP24* in HEK-293 and MCF-7 cells and their responsiveness to $1\alpha,25(OH)_2D_3$ over time (**A**). The cells were treated with 10 nM $1\alpha,25(OH)_2D_3$ for 2, 6 and 24 h, prior to the extraction of RNA. The dependence of the hormone responsiveness of the genes on VDR expression was investigated by RNAi inhibition experiments. For this purpose, the cells were transfected with unspecific control siRNA oligomers or with specific siRNAs against the VDR mRNA. The siRNA treatment time was 72 h. Silencing of VDR at protein level was verified by immunoblotting using whole-cell extracts (**B**). After siRNA treatment, the cells were further treated with 10 nM $1\alpha,25(OH)_2D_3$ for 3 h. The extracted RNA was reverse transcribed and analyzed by quantitative real-time PCR (**C**). Columns indicate the means of three independent cell treatments and the tips of the bars represent standard deviations. Two-tailed, paired Student's *t*-tests were performed and *P*-values ($^{*}P<0.05$, $^{**}P<0.01$, $^{***}P<0.001$) of the fold inductions at the respective time points were calculated in reference to time-matched vehicle-treated reference (A) or in comparison to transfection with siRNA specific to VDR mRNA (B).

regulation at 6 h could be observed. *VDIR* mRNA expression followed the *METTL1* expression in both cell lines. *CYP24* mRNA expression was significantly induced in both cell types.

In order to confirm the dependence of the regulation of the genes by $1\alpha,25(OH)_2D_3$ on VDR expression, VDR mRNA levels were inhibited by using specific siRNA oligomers (Figure 1B-C). Quantitative real-time PCR analysis showed that siVDR treatment significantly increased *CYP27B1* mRNA expression in HEK-293 cells but had no effect in MCF-7. For the expression of both the *METTL1* and the *VDIR* genes, no significant differences between control siRNA and VDR siRNA-treated cells could be observed, indicating that the changes in their mRNA expression (Figure 1A) are probably not caused by $1\alpha,25(OH)_2D_3$ treatment. When unspecific siRNA was used, $1\alpha,25(OH)_2D_3$ was able to up-regulate *CYP24* mRNA expression 3.5-fold in HEK-293 cells and 4000-fold in MCF-7 cells. However, when VDR siRNA was used, *CYP24* mRNA expression stayed at basal levels in HEK-293 cells and in MCF-7 an 80% decreased ligand effect was observed.

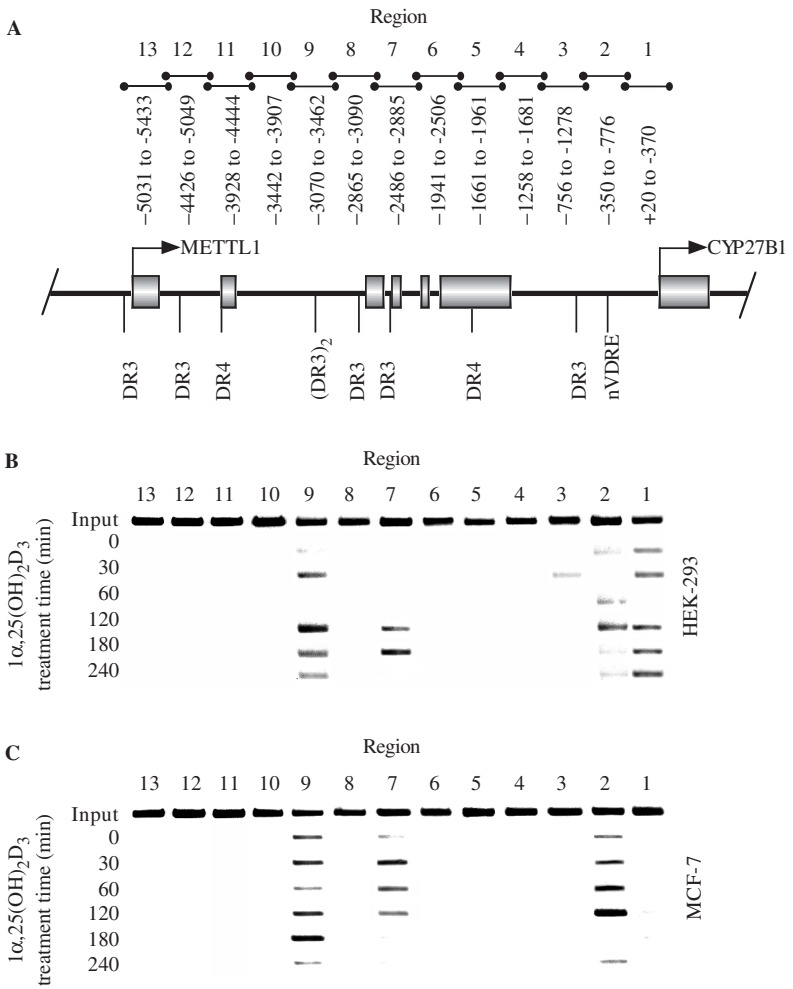

Figure 2. Recruitment of VDR to the *CYP27B1* promoter. Putative VDR-binding sites were determined by *in silico* screening by using the net-based program NUBIScan (33) (**A**). The analysis revealed nine putative VDREs within 5.4 kb upstream from the TSS of the *CYP27B1* gene. The gray cylinders indicate exons of the *METTL1* and *CYP27B1* genes. The location of PCR products obtained with the genomic primers (Table 2) used for ChIP assays are indicated above. Ligand-modulated binding of the VDR to these 13 overlapping regions of the human *CYP27B1* promoter was determined on chromatin templates obtained by ChIP assays. For this purpose, chromatin was extracted from HEK-293 (**B**) and MCF-7 (**C**) cells that had been treated for the indicated times with 10 nM $1\alpha,25(OH)_2D_3$ and precipitation was performed with an anti-VDR antibody. Representative agarose gels of 4–6 independent experiments are shown.

Taken together, the analysis of the *CYP24* gene expression confirms that both HEK-293 and MCF-7 cells have functional VDR-dependent $1\alpha,25(OH)_2D_3$ signaling. However, only in the kidney-derived HEK-293 cells, the *CYP27B1* gene is down-regulated by $1\alpha,25(OH)_2D_3$ via the VDR. Finally, the genes *METTL1* and *VDIR* appear not to be primary targets of the VDR.

Scanning the CYP27B1 promoter for VDR-binding sites

We scanned *in silico* the first 5.2 kb of the human *CYP27B1* promoter for putative VDREs utilizing the Internet portal NUBIScan (www.nubiscan.unibas.ch) (33) (Figure 2A). This screening revealed seven DR3-type and two DR4-type VDREs (Figure 2A). Interestingly, only one DR3-type VDRE was found within the first 1.7 kb of the promoter, to which previous studies were restricted (4,27–29). This region could be considered as the 'pure' promoter of the *CYP27B1* gene, since the *METTL1* gene is located only 1.2–5.4 kb upstream from its TSS. Thus, the eight other putative DR3- and DR4-type VDREs are located within *METTL1* gene.

Next we used chromatin from crosslinked $1\alpha,25(OH)_2D_3$-treated HEK-293 and MCF-7 cells, precipitated it with anti-VDR antibody and used the eluted chromatin template for a scanning with 13 overlapping genomic PCR primer pairs covering these 5.4 kb of the human *CYP27B1* promoter (Figure 2B and C). We observed VDR binding to the region of the established nVDRE (region 2: −350 to −776) but also to two additional regions located further upstream (region 7: −2486 to −2885 and region 9: −3070 to −3462). All three regions recruited VDR in a ligand-dependent fashion, reaching a maximum 120 min after onset of ligand treatment. Interestingly, three of the putative DR3-type VDREs lay within VDR-binding regions (Figure 2A).

In summary, in living HEK-293 and MCF-7 cells, VDR binds to three regions within the first 5.4 kb of the human *CYP27B1* promoter. The proximal region 2 contains the nVDRE, while the two distal regions 7 and 9 are located within the *METTL* gene and carry classical DR3-type VDREs.

Distal VDREs in the CYP27B1 promoter show direct VDR binding

The potential of the nVDRE of region 2, VDRE1 of region 7 and VDREs 2 and 3 of region 9 (for sequence, see Figure 3A) to associate with *in vitro*-translated VDR, RXR and VDIR (Figure 3B) were compared by gel shift analysis. The established DR4-type VDRE of the rat *Pit-1* gene (34) served as a positive control (Figure 3C). None of the four classical VDREs bound VDR or RXR alone, but with the exception of VDRE3 they bound, in a ligand-dependent fashion, VDR–RXR heterodimers (Figure 3C, E–G). VDIR bound efficiently to the nVDRE (Figure 3D), but did not interfere with the ligand-dependent VDR–RXR heterodimer formation on VDRE1, VDRE2 and the positive control (Figure 3C, E and F). Conversely, VDR and RXR did not associate on the nVDRE and did not interfere with VDIR binding to this element, either as monomers or as heterodimers (Figure 3D). Similarly, an anti-VDR antibody could not modulate the binding of VDIR on the nVDRE (Figure 3D), but it reduced the binding of VDR–RXR heterodimers to VDRE1, VDRE2 and the positive control (Figure 3C, E and F).

Taken together, *in vitro*, the nVDRE shows only association with VDIR protein, while VDRE1 and VDRE2 binds only VDR–RXR heterodimers. VDRE3 does not bind any of these proteins, suggesting that the binding of VDR to region 9 is mediated by VDRE2.

The ability of isolated CYP27B1 promoter regions to repress transcription

The functionality of the genomic regions 2, 7 and 9 of the human *CYP27B1* promoter was examined alone or together in a large promoter fragment by reporter gene assays in HEK-293 and MCF-7 cells (Figure 4). As a positive control, we used the proximal promoter of the human *CYP24* gene that contains a cluster of DR3-type VDREs. The latter promoter fragment was 6-fold inducible by $1\alpha,25(OH)_2D_3$ in HEK-293 cells and showed even a 30-fold inducibility in MCF-7 cells. In HEK-293 cells the basal activity of regions 2, 7 and 9 of the *CYP27B1* promoter was reduced by 15–40% by $1\alpha,25(OH)_2D_3$ treatment, but only the reductions of regions 2 and 9 were found to be statistically significant (Figure 4A). The large *CYP27B1* promoter fragment containing all three regions was even >50% reduced. In contrast, in MCF-7 cells, none of the four *CYP27B1* promoter constructs showed any significant response to stimulation with $1\alpha,25(OH)_2D_3$ (Figure 4B).

In summary, this analysis of the activity of the *CYP27B1* promoter parallels to the observation made on the level of mRNA expression (Figure 1), in that only in HEK-293 cells but not in MCF-7 cells, can a down-regulation by $1\alpha,25(OH)_2D_3$ be found. Interestingly, not only region 2 of the *CYP27B1* promoter, which contains the characterized nVDRE, supports this down-regulation but also region 9 (in which VDRE2 resides).

Ligand-dependent association of cofactor proteins with *CYP27B1* promoter regions

To further characterize the role of the *CYP27B1* gene promoter regions 2, 7 and 9, we performed an extensive ChIP analysis with antibodies against multiple VDR partner proteins in HEK-293 and MCF-7 cells (Figure 5). Region 6 of the *CYP27B1* promoter, which does not contain a VDRE, served as a negative control and a region covering the proximal promoter of the *CYP24* gene including its VDRE cluster was the positive control. In addition to VDR and RXR, the proteins were chosen to represent general chromatin activity (AcH3 and AcH4), gene activation (the CoAs SRC-1, SRC-2, SRC-3, CBP and pPolII) and gene repression (Sin3A and the CoRs SMRT and NCoR). At the three VDRE-containing regions of the *CYP27B1* promoter and in both cell types the acetylation level of histone H3 decreased in response to $1\alpha,25(OH)_2D_3$ treatment, while on the proximal promoter of the *CYP24* gene it significantly increased. However, at all four VDRE-containing regions the histone H4 acetylation level increased after ligand treatment.

In both cell types, VDR and RXR were associated ligand-dependently with the three VDRE-containing regions and the *CYP24* region, but not with the negative control region 6. The recruitment of HAT CBP, whose main substrate is the histone H3 tail, mirrored the changes in the histone H3 acetylation levels with the exception of the proximal promoter of the *CYP24* gene in HEK-293 cells, which did not bind CBP. In both cell types, pPolII associated strongly with the region 2 (containing the nVDRE) and reduced its binding after ligand treatment. Interestingly, in HEK-293 cells the same observation was made with region 7 (containing VDRE1), while in MCF-7 cells pPolII remained associated with the region even after ligand treatment. In both cell lines, region 9 and the negative control did not show any binding of PolII, while the proximal promoter of the *CYP24* gene demonstrated strong ligand-dependent recruitment of the polymerase.

The association of CoAs of the p160 family with different regions significantly differed in HEK-293 and MCF-7 cells. After ligand treatment in MCF-7 cells, SRC-1, SRC-2 and SRC-3 were recruited to the proximal *CYP24* promoter, while in HEK-293 cells this was the case only for SRC-1 and SRC-3. In HEK-293 cells, SRC-1 and SRC-3 bound only to region 2 of the *CYP27B1* promoter (and not to regions 6, 7 and 9) and dissociated from it after ligand stimulation. In contrast, in MCF-7 cells, SRC-1 bound constitutively to regions 2 and 7 (and not to region 9), while SRC-3 was strongly recruited by ligand treatment to regions 7 and 9 and in parallel partially dissociated from region 2.

In both cell lines, Sin3A bound constantly to region 2 through the time points analyzed and in HEK-293 cells, also to regions 7 and 9. After ligand stimulation, Sin3A dissociated in both cell lines from the proximal promoter fragment of the *CYP24* gene, while in parallel, in MCF-7

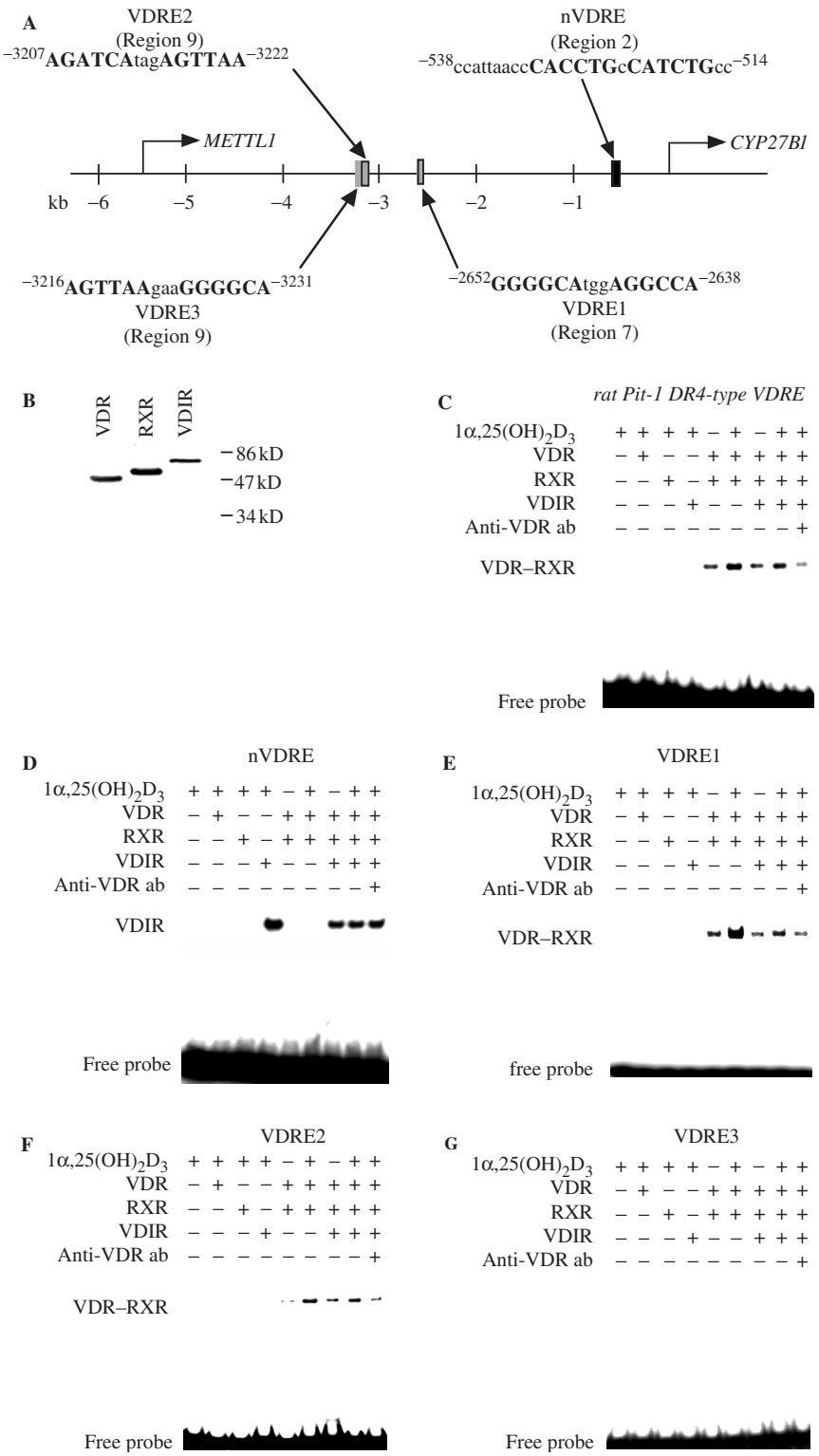

Figure 3. Recruitment of VDR–RXR heterodimers and VDIR to the VDREs found in the *CYP27B1* gene promoter. Sequence and location of VDREs within the human *CYP27B1* promoter (**A**). The hexameric core motifs within the DR3-type VDREs and the E-boxes within the nVDRE are shown in bold. Efficiency of *in vitro* translation of VDR, RXR and VDIR was examined by using ^{35}S-labeled proteins that were analyzed on a 12% denaturing polyacrylamide gel (**B**). Gel shift experiments were performed with *in vitro*-translated VDR, RXR and VDIR proteins in the presence or absence of 1 μM 1α,25(OH)$_2$D$_3$ on the established DR4-type VDRE of the rat *pit-1* gene (core sequence 5′-gaAGTTCAtgagAGTTCA-3′, **C**), the nVDRE (**D**) and the putative VDREs 1, 2 and 3 (**E–G**). Anti-VDR antibody was used to challenge the specificity of the protein–DNA complexes. The latter were resolved from free probe through 8% non-denaturing polyacrylamide gels. Representative gels are shown.

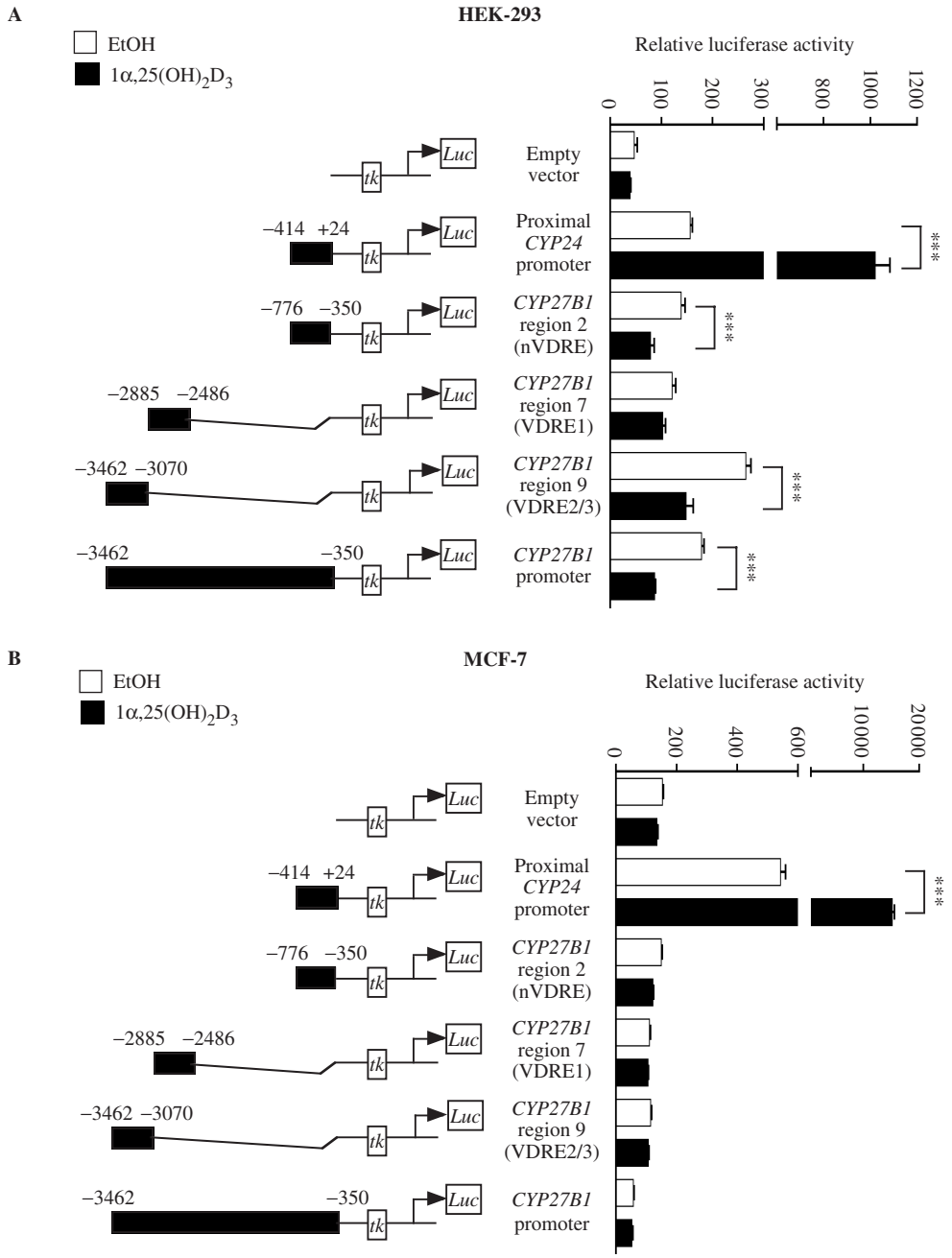

Figure 4. Functional analysis of the VDR-associated regions in the *CYP27B1* promoter. Regions 2, 7 and 9 of the human *CYP27B1* promoter were cloned alone or together (as found in the human genome) in front of thymidine kinase (*tk*) promoter driving the luciferase (*Luc*) gene. The proximal promoter of the human *CYP24* gene containing a cluster of DR3-type VDREs was used as a positive control and the empty reporter vector as a negative control. These reporter gene constructs were transfected together with an expression vector for VDR to HEK-293 (**A**) and MCF-7 (**B**) cells. Luciferase activity was determined after 16 h $1\alpha,25(OH)_2D_3$ treatment. Columns indicate the means of three independent experiments and the tips of the bars represent standard deviations. Two-tailed, paired Student's *t*-tests were performed and *P*-values ($^{***}P<0.001$) of the fold inductions were calculated in reference to vehicle-treated controls.

cells, it was recruited to region 7 and not at all to region 9. The CoR, SMRT was recruited by ligand in both cell lines to regions 2 and 7 and dissociated from the proximal *CYP24* promoter region. SMRT was in HEK-293 cells and was also recruited to region 9, a phenomenon not observed in MCF-7-cell-derived chromatin templates. Finally, in HEK-293 cells, after ligand treatment, NCoR1 was recruited to regions 2, 7 and 9, while in MCF-7 cells it was only recruited to region 7 and in parallel dissociated from regions 2 and 9. In both cell lines, NCoR1 dissociated from the proximal *CYP24* promoter.

Taken together, the ligand-dependent association and dissociation of cofactor proteins to the three VDR-binding regions of the *CYP27B1* promoter, in particular the CoAs SRC-1 and SRC-3 and the CoR, NCoR1, show significant differences between HEK-293 and MCF-7 cells.

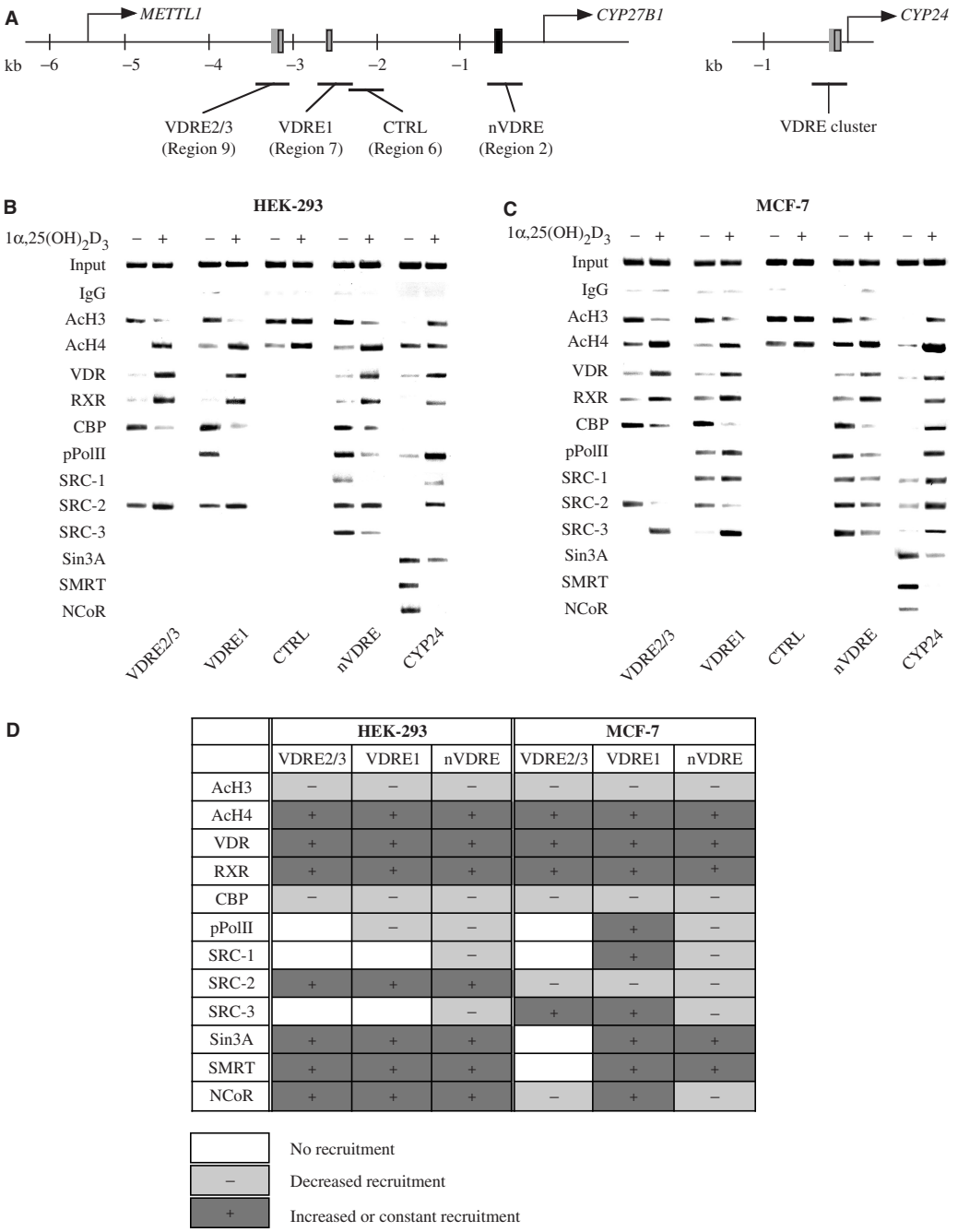

	HEK-293			MCF-7		
	VDRE2/3	VDRE1	nVDRE	VDRE2/3	VDRE1	nVDRE
AcH3	–	–	–	–	–	–
AcH4	+	+	+	+	+	+
VDR	+	+	+	+	+	+
RXR	+	+	+	+	+	+
CBP	–	–	–	–	–	–
pPolII		–	–		+	–
SRC-1			–		+	–
SRC-2	+	+	+	–	–	–
SRC-3			–	+	+	–
Sin3A	+	+	+		+	+
SMRT	+	+	+		+	+
NCoR	+	+	+	–	+	–

Figure 5. Ligand-induced recruitment of VDR partner proteins onto the *CYP27B1* promoter. Location of $1\alpha,25(OH)_2D_3$-responsive regions within the human *CYP27B1* and the human *CYP24* promoter (**A**). VDREs are indicated by gray boxes. Region 6 serves as a negative control, since it neither contains a VDRE nor bound VDR. Chromatin was extracted from HEK-293 (**B**) and MCF-7 (**C**) cells that had been treated for 0 or 120 min with 10 nM $1\alpha,25(OH)_2D_3$. The association of VDR and its partner proteins was monitored on the four VDRE-containing genomic regions and on the control region. PCR on input chromatin template served as a positive control and that from IgG-precipitated template as a specificity control. Three independent experiments were performed and representative PCR products are shown. The ChIP results are summarized in (**D**).

This may explain the differential transcriptional response of the *CYP27B1* gene in both cell lines to stimulation with $1\alpha,25(OH)_2D_3$.

Connectivity of the distal and proximal VDR-binding regions of the *CYP27B1* promoter

We used 3C assays in order to investigate, whether the distal regions 7 and 9 of the human *CYP27B1* promoter are directly connected with region 2 containing the nVDRE and/or region 1 including the TSS (Figure 6). The restriction enzyme HinfI was used to digest major parts of the DNA loops between the binding sites of genomic primers on the TSS (A), a control site (B), VDRE1 (C) and VDRE2/3. Under no conditions was a PCR product obtained with the genomic primers A and B, indicating that the control region was not looping to the

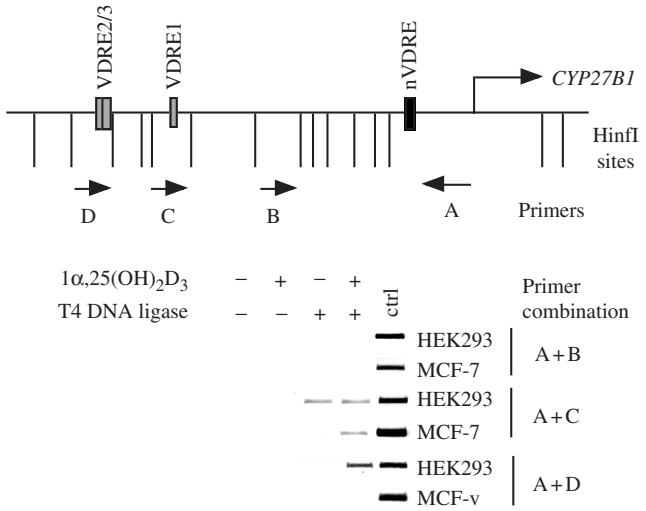

Figure 6. DNA looping connects distal and proximal *CYP27B1* promoter regions. Chromatin was extracted from HEK-293 and MCF-7 cells that had been treated for 120 min with 10 nM $1\alpha,25(OH)_2D_3$. The genomic DNA was digested with HinfI (recognition sites represented by vertical lines) and ligated with T4 DNA ligase. PCR was performed on purified genomic template with primer A in combination with primers B, C or D (location indicated by horizontal arrows). Digestions performed with a large subcloned *CYP27B1* promoter fragment provided templates for positive control PCR reactions. Representative agarose gels of the PCR products are shown.

TSS. In contrast, in MCF-7 cells VDRE1 containing-region (region 7) was ligand-dependently connected with proximal region (PCR fragment obtained by primers A and C) containing both the nVDRE and the TSS, while in HEK-293 cells this DNA looping occurred even in the absence of ligand. Moreover, only in HEK-293 cells VDRE2/3-containing region (region 9) looped ligand-dependently to the TSS and the nVDRE (PCR fragment obtained by primers A and D).

In summary, the 3C analysis indicated that in HEK-293 cells DNA looping between regions 1/2 and regions 7 and 9 takes place suggesting that the VDREs in these regions may act synergistically. Moreover, in HEK293 cells specifically, region 9 interacted with regions 1/2 only in the presence of hormone. This together with our previous reporter gene analysis indicates that region 9 contains a functional vitamin D-dependent repressor that is able to act together with the TSS/nVDRE-containing region to repress gene transcription. In contrast, in MCF-7 cells only a connection between regions 1/2 and region 7 was observed and this did not lead to gene repression.

DISCUSSION

The mechanism of negative gene regulation by nuclear receptors is still poorly understood, but the human *CYP27B1* gene and its down-regulation in the presence of $1\alpha,25(OH)_2D_3$ may be so far the most detailed model (4). Since the model takes account only the proximal promoter of the *CYP27B1* gene, we aimed in this study to test the hypothesis that also in the case of gene repression multiple response elements located in more distal regions may be involved in the regulation.

The distance between the TSSs of the neighboring genes *CYP27B1* and *METTL1* is only 5.4 kb (Figure 2A), with the *METTL1* gene being read in the same direction as *CYP27B1* (its last exon ends only 1.2 kb upstream of the TSS of the *CYP27B1*gene). Thus, the promoter of *CYP27B1* seems to be only 1.2 kb in size. Indeed, the studies of human and mouse *CYP27B1* promoters have so far considered only the first 1.7 kb upstream from the TSS of *CYP27B1* (4,27–29). Therefore, it is interesting that the combined results of our *in silico* screening and promoter ChIP scanning suggested that within the studied *CYP27B1* promoter region, two additional VDREs, located in regions 7 and 9 (being within introns of the *METTL1* gene) upstream from region 2 carrying the nVDRE. According to our ChIP scanning of the *CYP27B1* promoter, the time-dependent binding profile of VDR was similar both in MCF-7 cells and HEK-293 cells with one exception. In HEK-293 cells, the VDR seemed to associate with the described *CYP27B1* gene TSS stronger than in MCF-7 cells (Figure 2). Since region 1 possesses neither an nVDRE nor a regular VDRE, this may suggest that the protein bridge exists between the VDR-binding regions and the TSS in HEK-293, but not in MCF-7 cells.

According to Murayama and colleagues (4), the association of the VDR–RXR heterodimer to the nVDRE is not a direct binding to DNA, but occurs via the transcription factor VDIR. We found that *in vitro*-translated VDR–RXR heterodimers cannot bind to the nVDRE although *in vitro*-translated VDIR can (Figure 3). Interestingly, with the distal VDREs, reasonable VDR–RXR heterodimer association could be observed with VDRE1 and VDRE2 from regions 7 and 9, respectively. This did not apply to the neighboring VDRE3, suggesting that VDR is associated only with VDRE2 within region 9. The binding of the VDR–RXR complex to VDRE1 and VDRE2 was ligand dependent, but contrary to that of nVDRE, the binding may involve direct interactions with DNA sequences. Therefore, the new distal VDREs resemble positive VDREs, as has been previously described for most of the negative VDREs identified so far (10–12).

A reporter gene analysis of different *CYP27B1* promoter fragments (Figure 4) showed that both the regions containing the nVDRE and VDRE2/3 were able to repress gene activity in HEK-293 cells, but not in MCF-7 cells. In addition, a longer promoter fragment including both the nVDRE and VDRE2/3, an even more significant repression was achieved. Therefore, our results suggest that both nVDRE and VDRE2/3 are efficient negative regulators of the *CYP27B1* promoter and work in HEK-293 cells together in the repression of *CYP27B1* gene expression.

Our ChIP data suggested that the acetylation level of histone H3 tails was decreased in both cells in response to $1\alpha,25(OH)_2D_3$ (Figure 5). Interestingly, although the histone H3 acetylation levels decreased, the chromatin did not change to completely non-permissive form, because the acetylation status of the histone H4 at all regions remained constant or even increased after the

addition of $1\alpha,25(OH)_2D_3$. The acetylation level of histone H3 at control region remained constantly high and acetylation level of histone H4 increased. This suggests that a wide area of chromatin of distal *CYP27B1* promoter is permissive in both cells in the absence of ligand, which may be related to the high basal activity of *CYP27B1* gene. Addition of ligand results in local deacetylation of regions 7 and 9 together with region 2 thus leading to repression. Neither of these histone acetylation patterns is able to describe the cell-type-selective repression described here. However, it is possible that other forms of histone marking such as methylation, acting alone or in combination with the histone acetylation may be involved. It is also possible that tissue-selective factors may have to be present.

In both cell types, different transcription factors were associated with the nVDRE in a very similar fashion (Figure 5). Significant differences could be observed in the recruitment of pPolII, the CoAs SRC-1 and SRC-3 and the CoR NCoR. In MCF-7 cells, the VDRE1-containing region seemed to favor interactions with CoAs more than in HEK-293 cells. Contrary to this, the region containing VDRE2/3 seemed to recruit CoRs more efficiently in HEK-293 cells than in MCF-7 cells. One possible explanation is that the different cell lines possess differing levels of distinct cofactors. According to the GNF SymAtlas database (35), MCF-7 and HEK-293 cells differ significantly from each other with respect to expression of SRC-1, SRC-3, NCoR1 and HDAC2, where the respective CoAs are expressed more in MCF-7 cells, whilst NCoR1 and HDAC2 are more abundant in HEK-293 cells. Thus it is possible that, although the CYP27B1 promoter is similarly permissive in both cell types, concerning the binding of transcription factors, the repression of the gene is reached only in HEK-293 cells, because some important transcription factors are missing in MCF-7 cells. This could explain, at least in part, our ChIP data. Interestingly, the binding profiles of transcription factors at different regions were very similar, especially in HEK-293 cells. This suggests that it is possible that different regions may be connected with each other via chromatin looping and therefore the output of single antibody ChIP analysis of the distal and proximal regions actually represents the same super complex of transcription factors.

This hypothesis is supported by the fact that our 3C analysis confirmed that the proximal and distal regions of the human *CYP27B1* gene promoter are in contact with each other (Figure 6). From the results, it can be observed that in MCF-7 cells region 7 (containing VDRE1) is connected to the region containing the TSS in a ligand-dependent manner, but the region containing VDRE2/3 does not form any similar connections. In contrast to this, in HEK-293 cells, regions encompassing both VDRE1 and VDRE2/3 were connected with a region containing the TSS of the *CYP27B1* gene. The connection between the VDRE1-containing region and the proximal promoter was present both in the absence and in the presence of ligand. However, the most striking result was that VDRE2/3-containing region was only in contact with the proximal promoter when $1\alpha,25(OH)_2D_3$ was present.

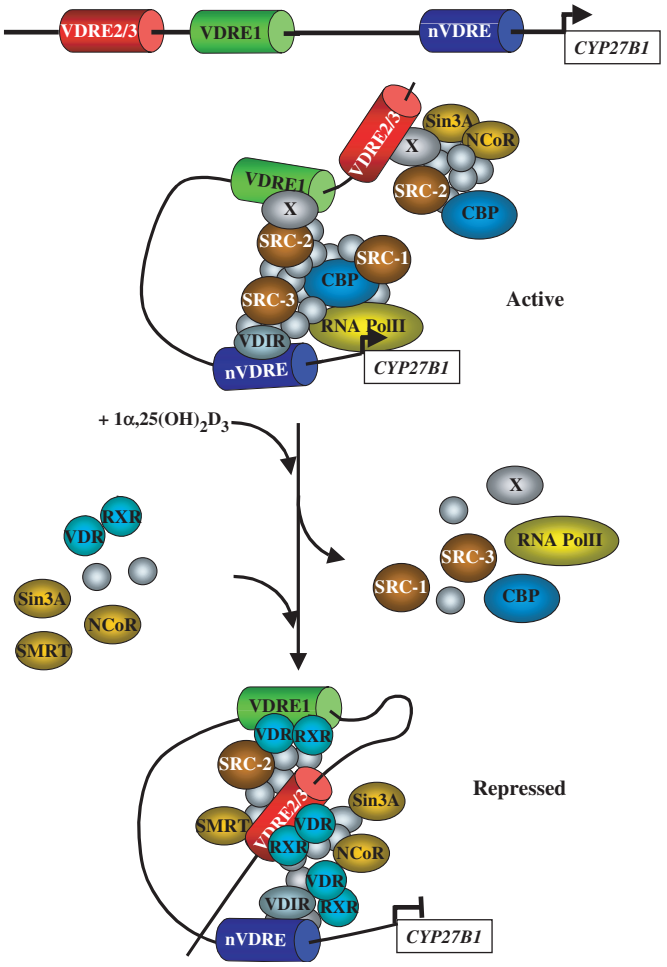

Figure 7. A model representing the crosstalk of distal and proximal promoter regions during the transcriptional regulation of the *CYP27B1* gene.

This suggests that VDRE1-containing region seems to be related more with basal (positive) transcriptional activity and that the VDRE2/3-containing region may have an important role in transcriptional repression. Please note that because there were no restriction-enzyme-cutting sites between the nVDRE and the TSS, it was impossible to determine exactly if VDRE1 or VDRE2/3 are connected to the nVDRE or TSS or both. In this case, the 3C analysis only reveals that the distal regions are connected with the proximal region that contains both the nVDRE and TSS.

In the light of our results presented here, we propose a model that may explain the role of distal VDREs in the transcriptional regulation of *CYP27B1* gene in HEK-293 cells (Figure 7). When the gene is active, chromatin looping brings the distal region, which includes VDRE1, close to the proximal promoter. Both regions associate with a common super complex of transcription factors that is broadly transcriptionally positive and includes CoAs such as SRC-1, SRC-2, SRC-3 and CBP. The nVDRE is connected via VDIR, but the anchoring transcription factor at VDRE1 is presently unknown.

We cannot either exclude the possibility that the ligand-independent looping happens via some other element that locates close to VDRE1. The HAT activity of CBP acetylates the histone H3 tails and thus keeps the chromatin at proximal promoter permissive for basal transcriptional machinery including pPolII. The region containing VDRE2/3 on the other hand is not involved in the transcriptional activation of the *CYP27B1* gene as can be inferred from its non-connectedness to the TSS-containing region in MCF-7 cells. However, it seems to recruit several transcription factors including repressive proteins, which are missing from the super complex associated with the nVDRE- and VDRE1-containing chromatin regions, selectively in HEK-293 cells. This suggests that a different complex is bound to this region, but the purpose of this complex is presently unknown as well as how the protein complex is associated with the region containing VDRE2/3. The addition of $1\alpha,25(OH)_2D_3$ results in the modulation of the super complex where activating transcription factors are replaced with repressing proteins. At the same time, the chromatin architecture changes and chromatin looping locates VDRE2/3 close to proximal promoter allowing it to associate with a common repressive super complex together with nVDRE and VDRE1.

In conclusion, we have revealed that the responsiveness of the *CYP27B1* gene to $1\alpha,25(OH)_2D_3$ is a cell-type-selective event that involves different combinations of multiple VDREs that act to recruit and interact with protein super complexes of differing transcriptional abilities. It is hoped that this work will allow us to understand better gene repression by nuclear receptors in general and the tissue-selective nature of the *CYP27B1* gene repression by $1\alpha,25(OH)_2D_3$ specifically.

ACKNOWLEDGEMENTS

We would like to thank Dr Shigeagi Kato for VDIR cDNA, Dr Job Dekker for help with the 3C technique, Dr Lise Binderup for $1\alpha,25(OH)_2D_3$ and Maija Hiltunen for help in cell culture. The Academy of Finland (Grant No. 00897) supported this research. Funding to pay the Open Access publication charges for this article was provided by Academy of Finland, Grant No. 00897.

Conflict of interest statement. None declared.

REFERENCES

1. Sutton,A.L. and MacDonald,P.N. (2003) Vitamin D: more than a "bone-a-fide" hormone. *Mol. Endocrinol.*, **17**, 777–791.
2. Nelson,D.R., Koymans,L., Kamataki,T., Stegeman,J.J., Feyereisen,R., Waxman,D.J., Waterman,M.R., Gotoh,O., Coon,M.J. *et al.* (1996) P450 superfamily: update on new sequences, gene mapping, accession numbers and nomenclature. *Pharmacogenetics*, **6**, 1–42.
3. Norman,A.W. (1971) Evidence for a new kidney-produced hormone, 1,25-dihydroxycholecalciferol, the proposed biologically active form of vitamin D. *Am. J. Clin. Nutr.*, **24**, 1346–1351.
4. Murayama,A., Kim,M.S., Yanagisawa,J., Takeyama,K. and Kato,S. (2004) Transrepression by a liganded nuclear receptor via a bHLH activator through co-regulator switching. *EMBO J.*, **23**, 1598–1608.
5. Henry,H. (2005)The 25-hydroxyvitamin D 1-a-hydroxylase. In Feldman,D., Pike,J.W. and Glorieux,F.H. (eds), *Vitamin D, 2nd edn*. Elsevier, Academic Press, pp. 69–83.
6. Townsend,K., Evans,K.N, Campbell,M.J., Colston,K.W., Adams,J.S. and Hewison,M. (2005) Biological actions of extra-renal 25-hydroxyvitamin D-1alpha-hydroxylase and implications for chemoprevention and treatment. *J. Steroid. Biochem. Mol. Biol.*, **97**, 103–109.
7. Cross,H.S. (2005)Vitamin D and colon cancer. In Feldman,D., Pike,J.W. and Glorieux,F.H. (eds), *Vitamin D, 2nd edn*. Elsevier, Academic Press, pp. 1709–1725.
8. Carlberg,C. and Polly,P. (1998) Gene regulation by vitamin D_3. *Crit. Rev. Eukaryot. Gene Expr.*, **8**, 19–42.
9. Quack,M. and Carlberg,C. (2000) Ligand-triggered stabilization of vitamin D receptor/retinoid X receptor heterodimer conformations on DR4-type response elements. *J. Mol. Biol.*, **296**, 743–756.
10. Demay,M.B., Kiernan,M.S., DeLuca,H.F. and Kronenberg,H.M. (1992) Sequences in the human parathyroid hormone gene that bind the 1,25-dihydroxyvitamin D_3 receptor and mediate transcriptional repression in response to 1,25-dihydroxyvitamin D_3. *Proc. Natl Acad. Sci. USA*, **89**, 8097–8101.
11. Falzon,M. (1996) DNA sequences in the rat parathyroid hormone-related peptide gene responsible for 1,25-dihydroxyvitamin D_3-mediated transcriptional repression. *Mol. Endocrinol.*, **10**, 672–681.
12. Kremer,R., Sebag,M., Champigny,C., Meerovitch,K., Hendy,G.N., White,J. and Goltzman,D. (1996) Identification and characterization of 1,25-dihydroxyvitamin D3-responsive repressor sequences in the rat parathyroid hormone-related peptide gene. *J. Biol. Chem.*, **271**, 16310–16316.
13. Xu,L., Glass,C.K. and Rosenfeld,M.G. (1999) Coactivator and corepressor complexes in nuclear receptor function. *Curr. Opin. Genet. Dev.*, **9**, 140–147.
14. Chen,J.D. and Evans,R.M. (1995) A transcriptional co-repressor that interacts with nuclear hormone receptors. *Nature*, **377**, 454–457.
15. Horlein,A.J., Naar,A.M., Heinzel,T., Torchia,J., Gloss,B., Kurokawa,R., Ryan,A., Kamei,Y., Soderstrom,M. *et al.* (1995) Ligand-independent repression by the thyroid hormone receptor mediated by a nuclear receptor co-repressor. *Nature*, **377**, 397–404.
16. Polly,P., Moehren,U., Baniahmad,A., Heinzel,T. and Carlberg,C. (2000) VDR-Alien: a novel, DNA-selective vitamin D(3) receptor-corepressor partnership. *FASEB J.*, **14**, 1455–1463.
17. Xu,W. (2005) Nuclear receptor coactivators: the key to unlock chromatin. *Biochem. Cell Biol.*, **83**, 418–428.
18. Chan,H.M. and LaThangue,N.P. (2001) p300/CBP proteins: HATs for transcriptional bridges and scaffolds. *J. Cell Sci.*, **114**, 2363–2373.
19. Chen,K.-S. and DeLuca,H.F. (1995) Cloning of the human 1α,25-dihydroxyvitamin D_3 24-hydroxylase gene promoter and identification of two vitamin D-responsive elements. *Biochim. Biophys. Acta*, **1263**, 1–9.
20. Hahn,C.N., Kerry,D.M., Omdahl,J.L. and May,B.K. (1994) Identification of a vitamin D responsive element in the promoter of the rat cytochrome P45024 gene. *Nucleic Acids Res.*, **22**, 2410–2416.
21. Kahlen,J.P. and Carlberg,C. (1994) Identification of a vitamin D receptor homodimer-type response element in the rat calcitriol 24-hydroxylase gene promoter. *Biochem. Biophys. Res. Commun.*, **202**, 1366–1372.
22. Zierold,C., Darwish,H.M. and DeLuca,H.F. (1995) Two vitamin D response elements function in the rat 1,25-dihydroxyvitamin D 24-hydroxylase promoter. *J. Biol. Chem.*, **270**, 1675–1678.
23. Sinkkonen,L., Malinen,M., Saavalainen,K., Väisänen,S. and Carlberg,C. (2005) Regulation of the human cyclin C gene via multiple vitamin D_3-responsive regions in its promoter. *Nucleic Acids Res.*, **33**, 2440–2451.
24. Väisänen,S., Dunlop,T.W., Sinkkonen,L., Frank,C. and Carlberg,C. (2005) Spatio-temporal activation of chromatin on the human CYP24 gene promoter in the presence of 1alpha,25-dihydroxyvitamin D_3. *J. Mol. Biol.*, **350**, 65–77.
25. Matilainen,M., Malinen,M., Saavalainen,K. and Carlberg,C. (2005) Regulation of multiple insulin-like growth factor binding protein genes by 1a,25-dihydroxyvitamin D_3. *Nucleic Acids Res.*, **33**, 5521–5532.

26. Zella,L.A., Kim,S., Shevde,N.K. and Pike,J.W. (2006) Enhancers located within two introns of the vitamin D receptor gene mediate transcriptional autoregulation by 1,25–dihydroxyvitamin D_3. *Mol. Endocrinol.*, **20**, 1231–1247.
27. Hendrix,I., Anderson,P.H., Omdahl,J.L., May,B.K. and Morris,H.A. (2005) Response of the 5′-flanking region of the human 25-hydroxyvitamin D 1alpha-hydroxylase gene to physiological stimuli using a transgenic mouse model. *J. Mol. Endocrinol.*, **34**, 237–245.
28. Ebert,R., Jovanovic,M., Ulmer,M., Schneider,D., Meissner-Weigl,J., Adamsk,J. and Jakob,F. (2004) Down-regulation by nuclear factor kappaB of human 25-hydroxyvitamin D_3 1alpha-hydroxylase promoter. *Mol. Endocrinol.*, **18**, 2440–2450.
29. Brenza,H.L., Kimmel-Jehan,C., Jehan,F., Shinki,T., Wakino,S., Anazawa,H., Suda,T. and DeLuca,H.F. (1998) Parathyroid hormone activation of the 25-hydroxyvitamin D_3-1alpha-hydroxylase gene promoter. *Proc. Natl Acad. Sci. USA*, **95**, 1387–1391.
30. Carlberg,C., Bendik,I., Wyss,A., Meier,E., Sturzenbecker,L.J., Grippo,J.F. and Hunziker,W. (1993) Two nuclear signalling pathways for vitamin D. *Nature*, **361**, 657–660.
31. Li,G., Walch,E., Yang,X., Lippman,S.M. and Clifford,J.L. (2000) Cloning and characterization of the human retinoid X receptor alpha gene: conservation of structure with the mouse homolog. *Biochem. Biophys. Res. Commun.*, **269**, 54–57.
32. Kemmis,C.M., Salvador,S.M., Smith,K.M. and Welsh,J. (2006) Human mammary epithelial cells express CYP27B1 and are growth inhibited by 25-hydroxyvitamin D-3, the major circulating form of vitamin D-3. *J. Nutr.*, **136**, 887–892.
33. Podvinec,M., Kaufmann,M.R., Handschin,C. and Meyer,U.A. (2002) NUBIScan, an in silico approach for prediction of nuclear receptor response elements. *Mol. Endocrinol.*, **16**, 1269–1279.
34. Rhodes,S.J., Chen,R., DiMattia,G.E., Scully,K.M., Kalla,K.A., Lin,S.C., Yu,V.C. and Rosenfeld,M.G. (1993) . A tissue-specific enhancer confers Pit-1-dependent morphogen inducibility and autoregulation on the pit-1 gene. *Genes Dev.*, **7**, 913–932.
35. Su,A.I., Cooke,M.P., Ching,K.A., Hakak,Y., Walker,J.R., Wiltshire,T., Orth,A.P., Vega,R.G., Sapinoso,L.M. *et al.* (2002) Large-scale analysis of the human and mouse transcriptomes. *Proc. Natl Acad. Sci. USA*, **99**, 4465–4470.